ELSEVIER

Polymer 41 (2000) 8449–8454

polymer

www.elsevier.nl/locate/polymer

Structure and physical properties of poly(butylene succinate)/cellulose acetate blends

T. Uesaka[a], K. Nakane[a,*], S. Maeda[b], T. Ogihara[a], N. Ogata[a]

[a]Department of Materials Science and Engineering, Fukui University, Bunkyo 3-9-1, Fukui 910-8507, Japan
[b]Department of Applied Chemistry and Biotechnology, Fukui University, Bunkyo 3-9-1, Fukui 910-8507, Japan

Received 14 January 2000; accepted 23 February 2000

Abstract

Polybutylene succinate (Bionolle) and cellulose triacetate (CTA) were solvent-cast blended with chloroform. Homogeneous blend films were obtained over a wide range of composition. The structure and properties of the blend films were investigated using various apparatuses. From Fourier transform infrared spectroscopy, wide-angle X-ray, and thermal measurements, it was found that the miscibility of Bionolle (BN) with CTA is excellent. In other words, in CTA-rich samples, it was found that BN molecules in the CTA matrix do not form a crystalline state, but forms an amorphous state. Therefore, the mechanical properties of the CTA-rich samples do not indicate the singularity before and after the melting point of pure BN. When CTA-rich samples were heated above the glass transition temperature of CTA, the BN molecules were eluted from the CTA matrix. © 2000 Elsevier Science Ltd. All rights reserved.

Keywords: Polybutylene succinate; Bionolle; Cellulose triacetate

1. Introduction

In recent years, the environmental situation of the earth is worse than that in old times. Waste matters of plastics are responsible for the worse environment because these materials are hard to dispose of. If all the conventional plastics were made from biodegradable polymers, the environmental problems would be reduced. However, these polymers are not widely used because not only are the polymers expensive, but also the range of the material selection suitable for various end-use purposes is limited; the number of the polymers with biodegradability is small. It is clear that the biodegradable polymers with various properties are highly in demand from now on. For the production of new materials, the polymer blend is an easy method. Therefore, we attempt to produce a new biodegradable composite material by using the blending technique.

Bionolle (BN) [1] is a biodegradable aliphatic thermoplastic polyester. This polymer is a semi-crystalline polymer and flexible as found from the structure. The polymer was designed to have the processibility of polyethylene with physical properties similar to those of polyethylene terephthalete.

Cellulose triacetate (CTA) is made from cellulose; all the six OH groups in the cellobiose units of cellulose are substituted by six $COOCH_3$ groups. It is usually an amorphous polymer and rigid as supposed from the molecular structure. Although CTA is not a biodegradable polymer originally, it could be changed to biodegradable cellulose by the hydrolysis. Therefore, CTA would be a biodegradable polymer in a wide sense.

Since there is a large difference in physical properties between BN and CTA, a material with new properties would be produced by blending these polymers. The blends of the cellulose-derivatives including cellulose with synthesized polymers have been attempted by many authors [2–8]. However, no work on the BN/CTA blend has been found in the literature except our preliminary study [9]. In this study, we investigate the structure and the thermal/mechanical properties of the BN/CTA blends in detail.

2. Experimental

2.1. Materials

Bionolle B1001 (BN) was supplied by Showa Highpolymer Co., Ltd (Tokyo, Japan). The number-average molecular weight is ca. 60 000. The chemical structure of the repeat unit is $-[O-(CH_2)_m-O-CO-(CH_2)_n-CO]_N-$. The parameters m and n were determined preliminarily using an

---

* Corresponding author. Tel.: +81-776-27-8639; fax: +81-776-27-8767.
E-mail address: nakane@matse.fukui-u.ac.jp (K. Nakane).

PII: S0032-3861(00)00206-8

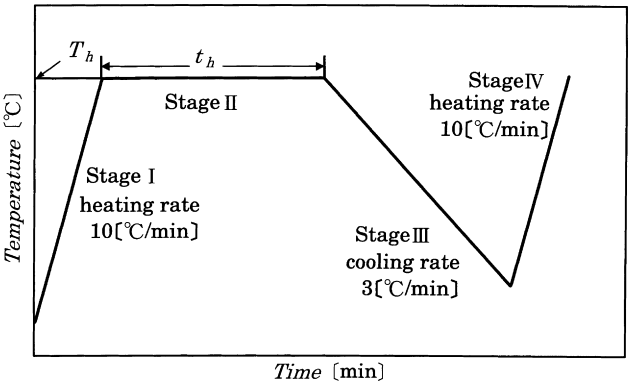

Fig. 1. The scanning program of DSC measurements.

ordinary NMR apparatus (JEOL LA-500). The values of *m* and *n* were found to be 4 and 2, respectively. Cellulose triacetate was also supplied by Mitsubishi Rayon Co., Ltd (Toyama, Japan); its molecular weight is unknown. Reagent grade chloroform was used without further purification.

2.2. Preparation of blends

Specified amounts of BN and CTA were placed in a beaker; the total amount of these materials was 1 g, and 20 ml of chloroform was added. After being stirred vigorously for about 2 h, the mixture became transparent, and then the solution was cast in a glass Petri dish. After chloroform was vaporized at 50°C, homogeneous films approximately 0.1 mm in thickness were obtained. The blend film containing a given amount of BN will be referred to as $\phi_{BN} = X$, where X represents the weight percentage of BN in the blend. The as-cast samples were also heat-treated at 200°C for 1 h. The heat-treated samples will be referred to as annealed samples.

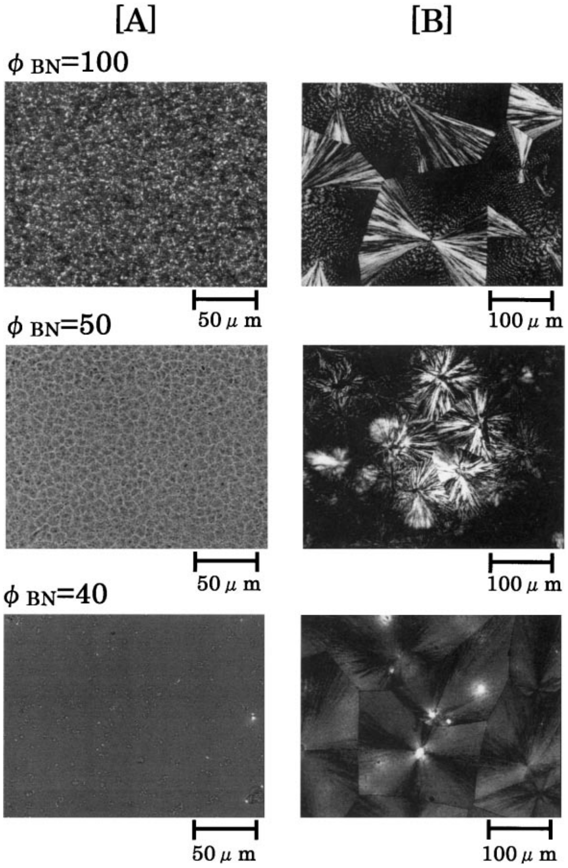

Fig. 2. Photographs of BN/CTA blends (as-cast (A), annealed (B)).

2.3. Characterization of blends

The structure of the blends was observed using a polarized optical microscope (Olympus model AX70TRF) with a heating device and a video recorder.

Fourier transform infrared spectra (FT-IR) were recorded in the reflection mode by a Shimadzu model 8300 FT-IR spectrometer with the resolving power of 2 cm^{-1}.

The X-ray diffraction curves of the blends were recorded by a Mac Science PM-20 with CuK_α radiation.

The thermal behavior of the blends was measured on a Shimadzu differential scanning calorimeter (DSC-60). The scanning program used in this study is shown in Fig. 1. The program consists of four stages and the thermal behavior of the blends at each stage will be discussed. The melting point, T_m, and heat of fusion, ΔH_m, were evaluated from a maximum position of the endothermic peak and its area on the DSC curves, respectively.

Dynamic mechanical analyses (DMA) of the blends were performed with a Rheometric Scientific RSAII Viscoelastic Analyzer. Temperature scans at 1 Hz frequency were carried out with a heating rate of 2°C/min. The glass transition temperature T_g is evaluated from the peak position of the tan δ vs. temperature curves.

The tensile tests for the blends were performed at room temperature on a Tensilon UTM-III tensile tester (Toyo Baldwin Co. Ltd.); the cross head speed was 10 mm/min and the initial gauge length was 50 mm.

3. Results and discussion

3.1. Structure of blends

The observation with naked eyes showed that the $\phi_{BN} \leqq 40$ films were quite transparent, while the $\phi_{BN} \geqq 50$ films were homogeneously opaque. Fig. 2 shows the photographs of the blends. Although small spherulites of BN can be seen in the as-cast $\phi_{BN} = 100$ and 50 samples, such spherulites cannot be seen in the as-cast $\phi_{BN} = 40$ sample; no BN crystallites could be seen under the crossed Nicols state. In the annealed $\phi_{BN} = 100$ sample, well-developed spherulites can be seen. On the other hand, in the annealed $\phi_{BN} = 50$ sample, undeveloped spherulites can be seen. This means that CTA restricts the formation of well-developed spherulites. It should be noted that the annealed $\phi_{BN} = 40$ shows the well-developed spherulitic structure, although the

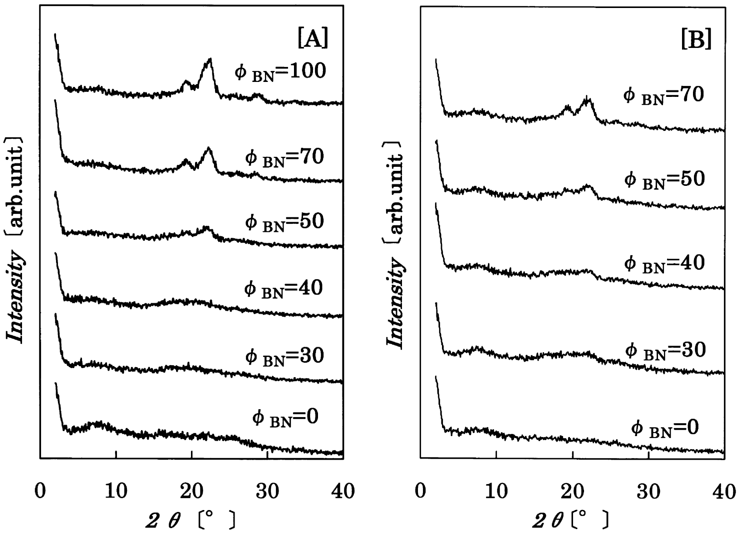

Fig. 3. X-ray diffraction curves of: (A) as-cast; and (B) annealed blends.

as-cast $\phi_{BN} = 40$ shows no BN spherulites. The well-developed BN spherulites seen in the annealed $\phi_{BN} = 40$ are formed from the BN molecules eluted to the surface of the blends; an evidence to support this idea will be described later.

Fig. 3 shows the X-ray diffraction intensity curves of the as-cast and annealed blends. Two intensity maximums originated from the BN crystallites can be seen at $2\theta \fallingdotseq 20°$ in the as-cast $\phi_{BN} \geqq 50$ samples. However, in the as-cast $\phi_{BN} \leqq 40$ samples, such maximums cannot be seen. This means that the BN molecules does not form the crystalline structure, but forms the amorphous state in the as-cast $\phi_{BN} \leqq 40$ samples. However, crystalline pattern can be seen in the annealed $\phi_{BN} = 40$ samples. This means that the crystallization of BN takes place in the annealing process of the $\phi_{BN} = 40$ sample.

Fig. 4 shows the results of FT-IR analysis of the as-cast and annealed blends. There is a difference between the peak position of carbonyl group of BN (1711 cm^{-1}) and that of CTA (1735 cm^{-1}). As seen in the magnified view, the two peaks appear separately in $\phi_{BN} = 50$ sample, although a single peak can be seen in $\phi_{BN} = 40$ sample. Moreover, the annealed $\phi_{BN} = 40$ exhibits two peaks separately. By taking into account these results and the fact that the crystallization of BN takes place during the annealing process, the appearance of a single peak is considered to mean that a hybrid structure of carbonyl groups of the BN and CTA components is formed. In other words, it seems that there is an interaction between the carbonyl group of BN and that of CTA. This interaction would be a reason that the BN molecules being miscible with the CTA molecules.

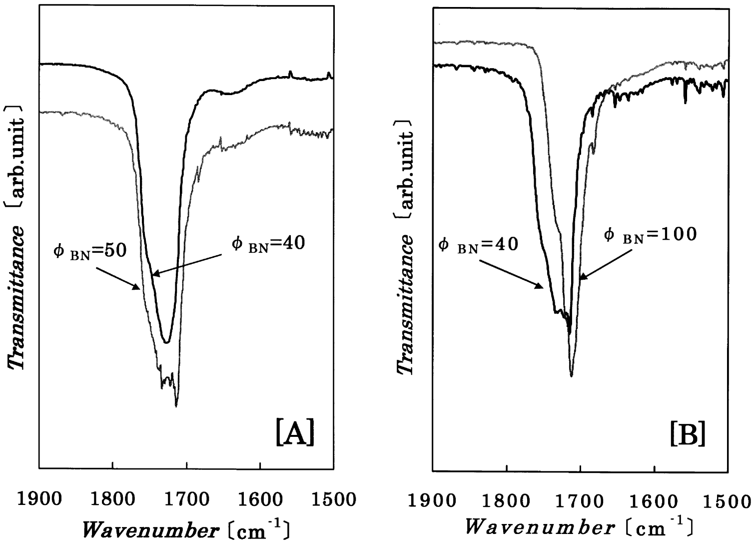

Fig. 4. FT-IR spectra of: (A) as-cast; and (B) annealed blends.

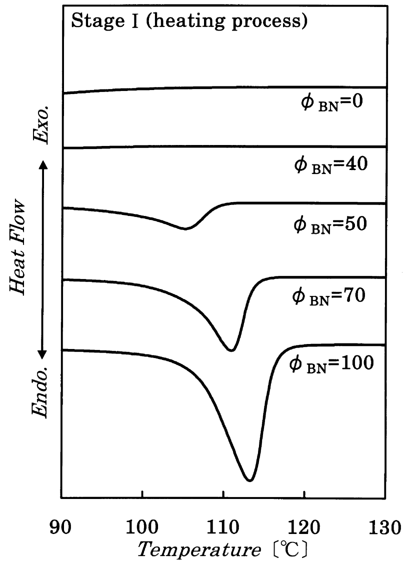

Fig. 5. DSC curves of as-cast blends at Stage I.

3.2. Thermal behavior of blends

Fig. 5 shows the DSC curves of the as-cast blends at Stage I (see Fig. 1). An endothermic peak can be seen at approximately 113°C in the $\phi_{BN} \geqq 50$ samples; this temperature corresponds to the melting point of BN. However, such a peak cannot be seen in the $\phi_{BN} \leqq 40$ samples. To discuss the effect of the BN content on the melting behavior of BN in detail, the values of T_m and ΔH_m were evaluated for each as-cast sample. The result is shown in Fig. 6. A straight solid line was drawn through the values of ΔH_m at $\phi_{BN} = 0$ and $\phi_{BN} = 100$, where the value for ΔH_m at $\phi_{BN} = 0$ was zero. It can be seen that T_m increases with increasing BN content (ϕ_{BN}). This result implies that larger BN crystallites are formed on increasing the BN content. It can be also seen that the experimental ΔH_m values deviate downward from the straight line on increasing the CTA content (decreasing the BN content). Especially, the value of ΔH_m cannot be observed at $\phi_{BN} \leqq 40$. These results mean that the introduction of the CTA molecules hinders the formation of the BN crystallites and the BN molecules in the CTA-rich samples ($\phi_{BN} \leqq 40$) in amorphous state. As discussed previously, a similar conclusion was obtained from the results of the X-ray measurement and optical observations.

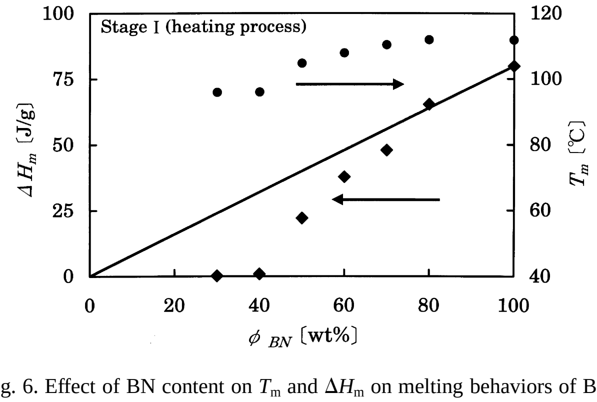

Fig. 6. Effect of BN content on T_m and ΔH_m on melting behaviors of BN.

The thermal behavior of the blends at Stage II (holding process as see Fig. 1) was also studied. Fig. 7 shows the DSC curves of the $\phi_{BN} = 30$ and $\phi_{BN} = 40$ samples. An exothermal peak can be seen for each sample. This result should be noted because such a peak was not observed for the $\phi_{BN} = 0$ and $\phi_{BN} = 100$ samples. To investigate the reason for the appearance of the peak, the peak position t_{max} was evaluated, and the Arrhenius plots of $1/t_{max}$ vs. the holding temperature T_h (see Fig. 1) were performed (Fig. 8). An almost linear relation between ln $1/t_{max}$ and T_h can be seen for both $\phi_{BN} = 30$ and $\phi_{BN} = 40$ samples. The activation energies calculated from the slopes are 2.74 and 2.24 kJ/mol for $\phi_{BN} = 30$ and 40, respectively. The linear relation suggests that the exothermal process is determined by a thermally activated molecular motion. Furthermore, to investigate the reason for the appearance for the exothermal peak, the melting behavior of $\phi_{BN} = 40$ samples at Stages I and II was video-recorded under the microscope using a heating rate 10°C/min (Fig. 9). No structural units can be seen in the micrographs recorded under 170°C. However, the micrographs recorded above 170°C indicate the structural changes; such a change was not observed for the $\phi_{BN} = 0$ and $\phi_{BN} = 100$ samples. From these results, the BN molecules are considered to be eluted from the CTA matrix when the blend is heated above T_g of CTA ($\fallingdotseq 200$°C); T_g of CTA will be discussed later. Well-developed spherulites seen in the annealed $\phi_{BN} = 40$ (see Fig. 2) seem to be formed from the BN molecules eluted from the CTA matrix. An exothermal peak would appear when the BN molecules are eluted and, consequently, form the BN droplets of the molten state on the surface of the films; excess surface energy of the molecules is released during the elution process.

The thermal behavior of Stage III is also studied. The crystallization temperature decreases on increasing the CTA content. This result implies that the existence of the CTA molecules does not enhance the crystallization of BN, but restricts it. During the crystallization of BN, the BN molecules should be aggregated, and this process would be hindered geometrically by the CTA molecules which are in frozen state, because T_g of CTA ($\fallingdotseq 200$°C) is markedly higher than the crystallization temperature of BN ($\fallingdotseq 90$°C).

3.3. Mechanical properties of blends

Fig. 10 shows the DMA curves of the BN/CTA blends. In the BN-rich samples, an abrupt change of storage modulus (E') can be seen at about 100°C; this temperature corresponds to T_m of BN. On the other hand, in the CTA-rich samples, such a change cannot be seen. In the CTA-rich samples, E' decreases on increasing the BN content and the decrease is marked at a high temperature range. Three

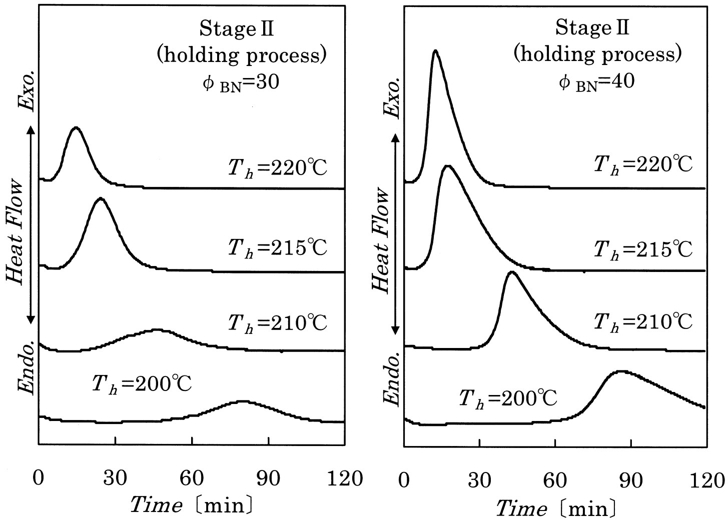

Fig. 7. DSC curves of $\phi_{BN} = 30$ and $\phi_{BN} = 40$ at Stage II.

maximums can be seen in the tan δ behavior of the BN-rich samples; the peaks at −32, 100 and 200°C correspond to T_g of BN, T_m of BN and T_g of CTA, respectively. T_g of BN cannot be seen in the CTA-rich samples. Although the tan δ at T_g of CTA decreases systematically with increasing BN content, T_g of CTA is independent of the BN content. These results suggest that the segmental motions of the CTA molecules are not restricted by the BN molecules. In other words, the interaction between the BN and CTA molecules seems to be weak at a high temperature.

Fig. 11 shows the effect of the BN content on the Young's modulus of the blends. This graph consists of three regions. That is, the Young's modulus decreases with increasing BN content up to about $\phi_{BN} = 40$, above which it remains almost constant up to about $\phi_{BN} = 70$, and then the value decreases. The Young's modulus is thought to decrease monotonically with increasing BN content because the modulus of BN is lower than that of CTA. Therefore, we have an interest in the fact that a constant Young's modulus is observed in the range from $\phi_{BN} = 40$ to $\phi_{BN} = 70$. In this region, the crystallization of the BN molecules is restricted by the existence of the CTA molecules (see Fig. 6). This leads to a decrease of the Young's modulus of the BN component with increasing CTA content. That is, the introduction of the CTA component does not simply lead to the increase of the Young's modulus of the blend. As discussed, two mutually competing effects of the addition of CTA may result in the constant Young's modulus in the range from $\phi_{BN} = 40$ to $\phi_{BN} = 70$.

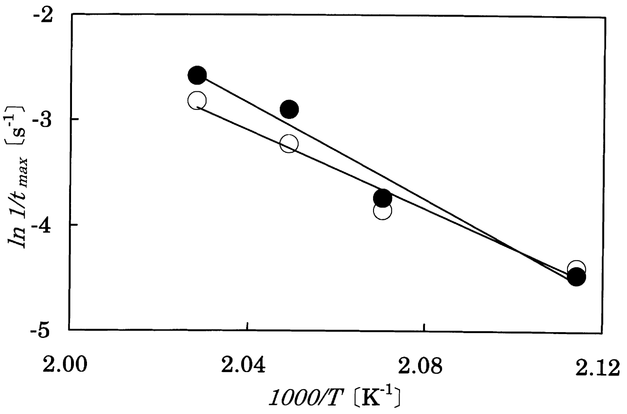

Fig. 8. Arrhenius plots of $1/t_{max}$ vs. T_h [●:$\phi_{BN} = 30$, ○:$\phi_{BN} = 40$].

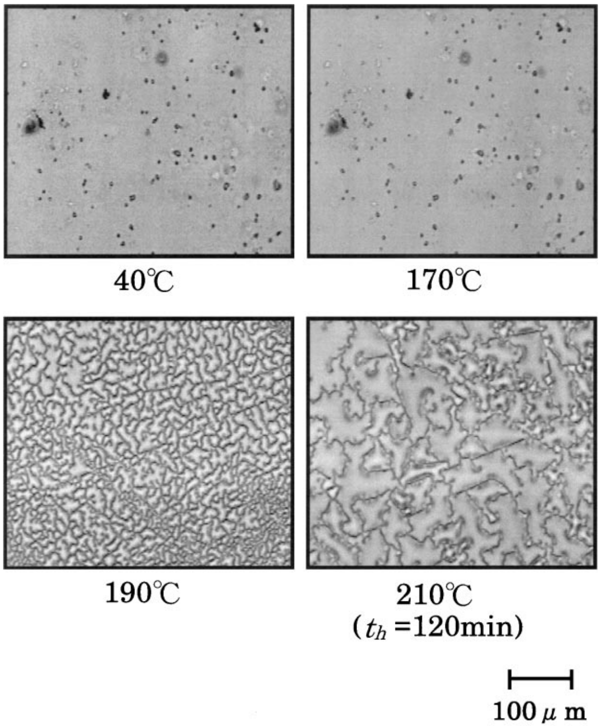

Fig. 9. Micrographs of melting process of $\phi_{BN} = 40$ at Stage I and II.

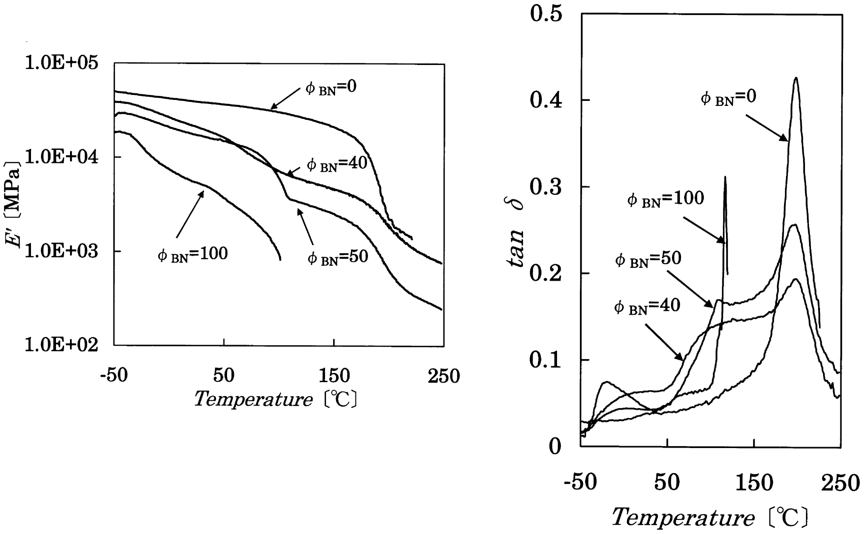

Fig. 10. DMA curves of BN/CTA blends.

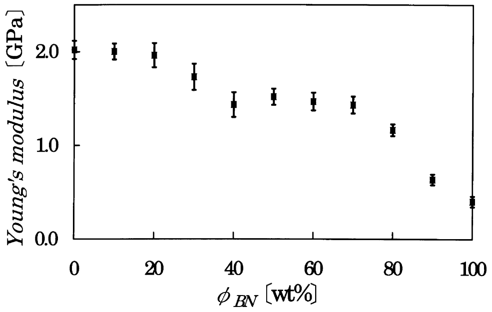

Fig. 11. Effect of BN content on Young's modulus of BN/CTA blends.

4. Conclusion

The structure and the thermal/mechanical properties of the BN/CTA blends have been investigated. The following conclusions are deduced from Section 3.

1. Homogeneous films are obtained from the blends of BN with CTA. That is, BN molecules are miscible with cellulose triacetate molecules.
2. The BN molecules in the CTA-rich samples are in an amorphous state.
3. In the CTA-rich samples, BN molecules are eluted from the inside of the blends to its surface when the blends are heated above T_g of CTA. During the elution, exothermal phenomenon is accompanied.
4. The existence of the CTA geometrically hinders the crystallization of BN.
5. In the CTA-rich samples, the melting behavior of the BN component is not observed on the dynamic mechanical measurement. This means that the blend is stable until the glass transition temperature of CTA.
6. The Young's modulus does not decrease monotonically with increasing BN content. That is, the region where the Young's modulus is independent of the BN content can be seen.

References

[1] Technical data sheet of Showa Highpolymer Co. Ltd, Japan.
[2] Nishio Y, St R, Manley J. Polym Engng Sci 1990;30:71.
[3] Nishio Y, Hirose N, Takahashi T. Polym J 1989;21:347.
[4] Nishio Y, Hirose N, Takahashi T. Sen-i Gakkaishi 1990;46:441.
[5] Buchanan CM, Gedon SC, White AW, Wood MD. Macromolecules 1992;25:7373.
[6] Buchanan CM, Gedon SC, White AW, Wood MD. Macromolecules 1993;26:2963.
[7] Saimos E, Dart RK, Dawkins JV. Polymer 1997;38:3045.
[8] Nagata N, Okana F, Sakai W, Tsutsumi T. Polym Sci Part A: Polym Chem 1998;36:1861.
[9] Ogata N, Kinari T, Kawakage S, Yanagawa T, Ogihara T, Yoshida N. Sen-i Gakkaishi 1996;52:277.